

Raman Spectroscopic and Electrochemical Characterization of Myoglobin Thin Film: Implication of the Role of Histidine 64 for Fast Heterogeneous Electron Transfer

Manliang Feng and Hiroyasu Tachikawa*

Contribution from the Department of Chemistry, Box 17910, Jackson State University, Jackson, Mississippi 39217-0510

Received August 17, 2000. Revised Manuscript Received January 2, 2001

Abstract: Myoglobin (Mb) thin films formed on various substrates have been characterized by using Raman spectroscopy, reflectance absorbance FT-IR, UV–vis absorption spectroscopy, and electrochemical methods. Raman spectra were obtained upon excitation within the Soret band as well as α – β bands. The spin state marker bands observed from the Mb film in the 1550–1630 cm^{-1} region (excitation at 514.5 nm) are $\sim 20 \text{ cm}^{-1}$ higher than those of aqueous metMb having the high spin state. The 1210 cm^{-1} band (methine bridge C–H vibration) also shifts to 1240 cm^{-1} upon the formation of the film. These results indicate that the heme iron of myoglobin in the film is the ferric low-spin state, and the iron atom is pulled to the heme plane. A comparison of the Raman spectra of the Mb film with that of an Mb-imidazole derivative leads to the conclusion that the distal histidine is responsible for the change in the spectral characteristics. The escape of water from the sixth position upon the formation of the Mb film may result in a conformational change at the heme distal pocket: the histidine residue at the E7 helical position (H64) moves toward the central iron and is coordinated with it through the N on the imidazole ring. These structural features facilitate the fast electron transfer between the thin protein film and the electrode. Distal histidine may serve as an electron-transfer pathway as it does in cytochrome c.

Introduction

Myoglobin (Mb) is a small heme protein found in cardiac and red skeletal muscle tissues for oxygen storage and transport.^{1,2} It contains a single polypeptide chain of 153 amino acid residues and a single electroactive iron porphyrin IX ring as the prosthetic group, and its molecular weight is $\sim 17\,000$.³ The polypeptide chain provides a nonpolar pocket, through appropriate folding, to accommodate and stabilize the porphyrin ring that is coupled to the polypeptide chain through the N on the imidazole ring of H93.^{4–6}

Electrochemical methods are useful tools for studying the intrinsic redox properties of heme proteins and provide a better understanding of the electron-transfer mechanism in biological systems. However, the direct electron transfer of these proteins at unmodified electrodes is extremely slow. In the case of Mb a slow electron transfer ($\sim 10^{-5} \text{ cm/s}$) was observed at a tin-doped indium oxide electrode.⁷ Considerable efforts have been made to explore methods that can increase the electron transfer between the heme protein and the electrode. The two most commonly used methods include modifying the electrodes with mediators and employing promoter molecules which can induce the proteins to assume an orientation to the electrode that favors

rapid electron transfer.⁸ Rusling and co-workers reported the direct electron transfer between electrodes and aquo-metMb incorporated in a variety of insoluble liquid crystal surfactant films on a pyrolytic graphite (PG) electrode.^{9–12} Electron transfer rates of Mb in these films were up to 1000-fold higher than that between a bare electrode and Mb in solution. Surfactants were arranged in stacked bilayers similar to lipid membranes where Mb was preferentially oriented and retained its native structure.⁹ A similar method was used to study the direct electron transfer of hemoglobin (Hb) at carbon electrodes.⁸ These film electrodes were also used to study the catalytic reduction of organohalide pollutants, nitrite, and nitric oxide (NO).^{13–15} We have recently observed that an Mb thin film covered with Nafion (Mb-Nafion) on a glassy carbon (GC) electrode (or ITO electrode) shows a fast electron transfer between the heme and the GC electrode which is similar to that observed in surfactant films. The Mb-Nafion film electrode also catalyzed the reduction of dioxygen and NO.¹⁶ This type of electrode, which is easy to prepare and is very stable, may

(1) Wittenberg, B. A.; Wittenberg, J. B.; Caldwell, P. R. B. *J. Biol. Chem.* **1975**, *250*, 9038–9043.

(2) Wittenberg, B. A.; Wittenberg, J. B. *Proc. Natl. Acad. Sci. U.S.A.* **1987**, *84*, 7503–7507.

(3) Edmundson, A. B.; Hirs, C. H. W. *J. Mol. Biol.* **1962**, *5*, 663–682.

(4) Kendrew, J. C.; Watson, H. C.; Strandberg, B. E.; Dickerson, R. E.; Phillips, D. C.; Shore, V. C. *Nature* **1961**, *190*, 666–670.

(5) Takano, T. *J. Mol. Biol.* **1977**, *110*, 537–568.

(6) Takano, T. *J. Mol. Biol.* **1977**, *110*, 569–584.

(7) King, B. C.; Hawkrige, F. M. *J. Electroanal. Chem.* **1987**, *237*, 81–92.

(8) Ciureanu, M.; Goldstein, S.; Mateescu, M. A. *J. Electrochem. Soc.* **1998**, *145*, 533–541.

(9) Rusling, J. F.; Nassar, A.-E. F. *J. Am. Chem. Soc.* **1993**, *115*, 11891–11897.

(10) Nassar, A.-E. F.; Willis, W. S.; Rusling, J. F. *Anal. Chem.* **1995**, *67*, 2386–2392.

(11) Rusling, J. F.; Nassar, A.-E. F. *Langmuir* **1994**, *10*, 2800–2806.

(12) Nassar, A.-E. F.; Narikiyo, Y.; Sagara, T.; Nakashima, N.; Rusling, J. F. *J. Chem. Soc., Faraday Trans.* **1995**, *91*, 1775–1782.

(13) Nassar, A.-E. F.; Bobbitt, J. M.; Stuart, J. D.; Rusling, J. F. *J. Am. Chem. Soc.* **1995**, *117*, 10986–10993.

(14) Lin, R.; Bayachou, M.; Greaves, J.; Farmer, P. J. *J. Am. Chem. Soc.* **1997**, *119*, 12689–12690.

(15) Bayachou, M.; Lin, R.; Cho, W.; Farmer, P. J. *J. Am. Chem. Soc.* **1998**, *120*, 9888–9893.

be useful for studying redox reactions of other heme proteins and for developing biosensors for the determination of such molecules as O₂, NO, and organohalide pollutants.¹³ However, there are several questions that need to be answered if one wants to use this type of electrode for elucidating reactions between heme proteins and other molecules by electrochemical methods: (1) Does Mb remain in the native form when the film is formed on the electrode surface? (2) Will covering the Mb film with Nafion affect the conformation of Mb? (3) Why is the electron transfer between Mb and the electrode at the Mb-Nafion/GC much faster than that of Mb in the solution at the bare GC electrode?

In the present study, an Mb film formed from an Mb solution (phosphate buffer) is characterized by using resonance Raman, FT-IR, and UV-vis absorption spectroscopies to obtain structural information for explaining the observed fast electron transfer between Mb and the electrode. Resonance Raman (RR) spectroscopy, which uses laser excitation in the electronic absorption bands producing a large enhancement of Raman scatterings for vibrational modes of chromophores, has been used as a probe for obtaining the structural information of biological molecules. RR spectra of heme proteins and their derivatives have been studied extensively, and the correlation between the spectra and structures of the heme group has been well established.^{17–21} RR spectroscopy has also been used to elucidate the interactions between the heme and its axial ligand^{22,23} as well as the conformational change of heme proteins.²⁴ Spectroscopic data obtained in the present experiments indicate that at the E7 helical position the distal histidine (H64), which plays a key role in ligand binding at the sixth position,^{25–27} moves toward heme iron and interacts with the prosthetic group through the imidazole side chain. This conformational change leads to the alteration of the spin state of iron from high in solution to low in the film, which should contribute to the fast electron transfer because of the involvement of the same spin states in the redox reaction. It also leads to the alteration of the distal pocket H-bonding network that should reduce the activation energy for the electron transfer. In addition, the imidazole group of the distal histidine may also function as an effective pathway for electron transfer due to the overlap of the p π orbital of imidazole with the d orbital of the iron atom. The conclusions obtained by these spectroscopic data are consistent with the cyclic voltammetric (CV) data showing a much higher electron-transfer rate in the film than in solution. A reflectance-absorbance infrared spectroscopic

study suggests that Mb in the film may still retain the essential features of its native structure.

Experimental Section

Preparation of Mb Films. Myoglobin (Mb) from horse skeletal muscle (Sigma) was dissolved in a 0.1 mol/L phosphate buffer (pH 7.4). The protein concentration was 5×10^{-4} mol/L. Myoglobin solutions were filtered through Whatman filters (0.2 μ m pore size) to remove undissolved impurities. The myoglobin-imidazole derivative was prepared from metMb by adding imidazole up to a minimal saturated concentration. Mb films were cast on various substrates including a quartz plate, gold, silver, platinum, and GC by pipetting 20 μ L of a 5×10^{-4} mol/L metMb solution onto the substrates followed by gradual evaporation of the solvent at room temperature. The final film covers an area of ~ 6 mm². For the electrochemical experiment, the film was formed on the GC electrode (Cypress, 1 or 1.5 mm diameter) and was further covered with a thin layer of Nafion. Before casting the protein films, the substrate electrodes were successively polished by using 15, 9, 6, 3, and 1 μ m METADI diamond polishing paste (Buehler) and a 0.05 μ m GAMMA Micropolis II Deagglomerated alumina suspension (Buehler) followed by supersonic washing in deionized and doubly distilled water.

Raman Spectroscopy. Raman spectra were recorded with two Raman systems. The first system consisted of an Instruments S.A. model Triax 180 spectrograph coupled with a Kaiser model HFPH-S-514.5 fiber optic probehead for both laser propagation and signal collection. A 1200 gr/mm grating was used in the spectrograph. This system is optimized for 514.5-nm excitation (Spectra-Physics model 171 Ar⁺ laser). The second Raman system consisted of a Spex model 1877 triple spectrometer interfaced with an Olympus model BH-2 microscope. This system was used for 406.7-nm excitation (Spectra-Physics model 171 Kr⁺ laser). Each system was equipped with a CCD detector and was calibrated with a standard argon lamp by using the software of SpectraMax for Windows 2.5 (Instruments S.A.). The deviation in the measured band frequencies is less than ± 5 cm⁻¹. All Raman experiments were performed in a 180° backscattering geometry. The laser powers at the samples were adjusted to 10 (for 514.5-nm excitation) and ~ 1 mW (for 406.7-nm excitation), respectively. To avoid laser-induced damage of the proteins, samples were placed on a spin stage or protected with a stream of cold nitrogen. To avoid damaging the Mb power sample, the laser beam was defocused (~ 4 -mm diameter) with a beam expander and Raman scattering was collected directly into the filter stage of the triple spectrometer. The spectrum was recorded with a 30-s accumulation time, and 15 repetitively measured spectra were averaged to improve the quality of the spectrum. Isotopic substitution experiments were conducted by dissolving Mb in H₂¹⁸O (Aldrich, 95 atom % ¹⁸O). The Mb film was also formed from this solution. To prevent the exchange of ¹⁸O by ¹⁶O in the atmosphere, isotopic substitution experiments were conducted under the protection of N₂.

FT-IR Spectroscopy. The IR spectra of the Mb film and as-received Mb on gold or GC surfaces were obtained by using a Nicolet model Nexus 670 FT-IR spectrometer with a model Continu μ m microscope and an MCT detector in reflectance mode at 2 cm⁻¹ resolution. As-received Mb samples were prepared by physical dispersion of commercial Mb solid on the substrate and the spectra were collected from a small piece of solid that lay parallel to the surface having a thickness similar to that of the film. To obtain good-quality spectra, 64 interferograms were co-added. Freshly polished substrates (gold or GC) were used as a background.

UV-Vis Absorption Spectroscopy. The absorption spectra of the Mb solution, Mb film, and as-received Mb powder were recorded on a Varian model Cary 3E spectrophotometer. The absorption spectra of each sample were obtained before and after Raman measurements and were used as references to monitor sample damage during the Raman experiments.²⁸ The UV-vis spectra of Mb were unaffected by the exposure to the laser beam during the Raman experiments.

Electrochemical Measurements. A CH Instruments model CHI 440 electrochemical workstation was used for recording cyclic voltammetry.

(16) Chou, J.; Tachikawa, H. *Abstracts of Papers*; 195th Meeting of the Electrochemical Society, Seattle, WA; Electrochemical Society: Pennington, NJ, 1999; Abstract 993, Vol. 99-1.

(17) Spiro, T. G.; Streckas, T. C. *J. Am. Chem. Soc.* **1974**, *96*, 338–345.

(18) Asher, S. A.; Vickery, L. E.; Schuster, T. M.; Sauer, K. *Biochemistry* **1977**, *16*, 5849–5856.

(19) Spiro, T. G.; Stong, J. D.; Stein, P. *J. Am. Chem. Soc.* **1979**, *101*, 2648–2655.

(20) Callahan, P. M.; Babcock, G. T. *Biochemistry* **1981**, *20*, 952–958.

(21) Hirota, S.; Ogura, T.; Appelman, E. H.; Shinzawa-Itoh, K.; Yoshikawa, S.; Kitagawa, T. *J. Am. Chem. Soc.* **1994**, *116*, 10564–10570.

(22) Tsubaki, M.; Srivastava, R. B.; Yu, N.-T. *Biochemistry* **1982**, *21*, 1132–1140.

(23) Tomita, T.; Hirota, S.; Ogura, T.; Olson, J. S.; Kitagawa, T. *J. Phys. Chem. B* **1999**, *103*, 7044–7054.

(24) Smulevich, G.; Miller, M. A.; Kraut, J.; Spiro, T. G. *Biochemistry* **1991**, *30*, 9546–9558.

(25) Bellelli, A.; Antonini, G.; Brunori, M.; Springer, B. A.; Sligar, S. G. *J. Biol. Chem.* **1990**, *265*, 18898–18901.

(26) Rohlf, R. J.; Mathews, A. J.; Carver, T. E.; Alson, J. S.; Springer, B. A.; Egeberg, K. D.; Sligar, S. G. *J. Biol. Chem.* **1990**, *265*, 3168–3176.

(27) Schulze, B. G.; Evanseck, J. D. *J. Am. Chem. Soc.* **1999**, *121*, 6444–6454.

(28) Asher, S. A.; Schuster, T. M. *Biochemistry* **1981**, *20*, 1866–1873.

grams (CVs) of the Mb film electrode and Mb derivatives. The three-electrode cell consisted of a saturated Ag/AgCl reference electrode (Ag/AgCl), a Pt wire auxiliary electrode, and a GC disk working electrode (Cypress, 1- or 1.5-mm diameter). The buffer solution in the cell was purged with nitrogen gas for at least 30 min before the experiment and was kept under positive pressure of nitrogen gas during the experiment.

Results and Discussions

Raman Spectroscopy. The heme group of Mb has two distinct electronic transitions which give rise to bands in the absorption spectrum near 400 (Soret) and 500–550 nm (α - β bands). Laser excitation in the Soret and α - β band regions brings out different sets of Raman bands via different resonance scattering mechanisms.¹⁷ In the present study, a 406.7-nm excitation from a Kr⁺ laser and a 514.5-nm excitation from an Ar⁺ laser were used. These sources are within the Soret and α - β band regions of Mb, respectively.

The Raman spectrum of Mb in buffer solution excited with the 514.5 nm line of an Ar⁺ laser shows a series of Raman bands mostly in the higher frequency region. These bands were assigned mainly to the bending vibration of the C–H bonds of the methine bridges and stretching vibrations of the pyrrolic C–C and C–N bonds of the porphyrin ring.^{29,30} Their frequencies are influenced by the conjugative interaction of π electrons between the central metal ion and the porphyrin ring; the oxidation state of iron and the properties of the sixth ligand may affect the conjugative effects between iron and porphyrin and should thus be reflected in the Raman spectra. It is widely accepted that the intense peak at \sim 1360–1370 cm⁻¹, which is assigned to the C–N vibration,³¹ is sensitive to the oxidation state of the heme iron,^{17,29–33} for ferrous Mb this band appears at \sim 1360 cm⁻¹ while for ferric metMb it appears at \sim 1374 cm⁻¹. Bands in the 1500–1630 cm⁻¹ region correspond to the vibration of the C–C bond of the porphyrin ring; the 1565 cm⁻¹ band is sensitive to the spin state of the heme iron,¹⁶ and the band at 1623 cm⁻¹ is sensitive to both spin and oxidation states.³³ The frequencies of these vibrational modes increase with an increase of the ratio of low spin to high spin. The frequency of the polarized mode in this region was also found to correlate with the porphyrin core size.²⁰

The Raman spectrum of metMb in a phosphate buffer is shown in Figure 1a. The intense bands at 1374, 1565, and 1623 cm⁻¹ indicate that iron is in the ferric and high-spin state. Figure 1b shows the Raman spectrum of the Mb thin film on a quartz plate. The Mb thin film on other substrates including gold, silver, platinum, and GC shows basically the same Raman spectra as that of the Mb film on a quartz plate. Some distinct differences can be recognized in the two spectra shown in Figure 1: The spin marker band at 1565 cm⁻¹ from the solution sample shifted to 1592 cm⁻¹ in the spectrum from the film. Likewise, the band at 1623 cm⁻¹ shifted to 1643 cm⁻¹, and the band at 1210 cm⁻¹, which corresponds to a methine C–H in-plane bending vibration, shifted to 1240 cm⁻¹. However, the oxidation state marker band (1374 cm⁻¹) remained at the same position. These results indicate that the Mb film is in the ferric low-spin state and the iron atom lies in the heme plane rather than being displaced by

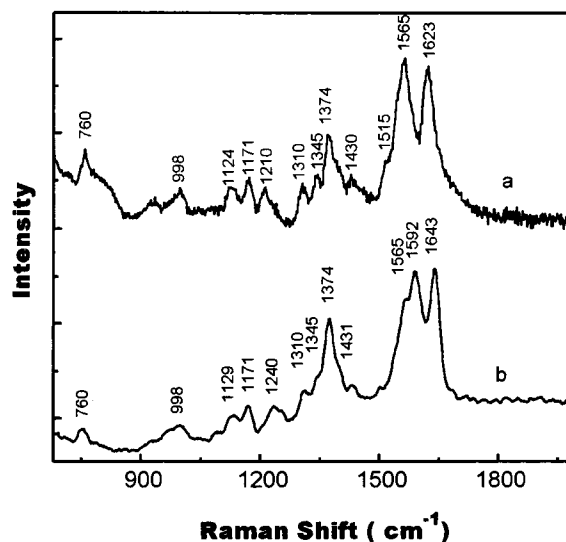


Figure 1. Resonance Raman spectra of (a) aqueous metMb and (b) Mb film. $\lambda_{\text{ex}} = 514.5$ nm.

\sim 0.4 Å out of the heme plane, which is the case for aqueous metMb.³⁴ Consequently, one can expect a strong ligand coordination to iron at the sixth position in the Mb film.

To further confirm this result, a 406.7 nm excitation was used to obtain Raman spectra from both aqueous metMb and Mb films. The Soret band dominates the scattering process with this excitation. In addition to the oxidation and spin marker bands in the high-frequency region, a 406.7 nm excitation brought out a set of bands in the low-frequency region (see Figure 2). These Raman bands result mostly from an Fe–N (pyrrole and proximal histidine) bond stretch and heme deformation.³⁵ The relative intensities of bands C, D, and I (heme deformation) constitute indicators of the doming state of the heme and of the spin state of the iron atom. The pure high spin yields a doublet at band A, while the low-spin derivative presents only one peak in this region. Another spectral feature that reflects the spin state is the intensity ratio of band C to D: for the high-spin complex this ratio is <1 , while for low-spin complex the ratio is >1 .

The Raman spectrum of aqueous metMb [Figure 2A(a)] showed two bands at 249 and 272 cm⁻¹ in the region of band A, and the relative intensity of band D was higher than that of band C. The spectrum of the Mb film, on the other hand, showed a single band at 272 cm⁻¹ in region A and the relative intensity of band C was higher than that of band D. These spectroscopic data again indicate that the spin state of the iron atom in Mb was changed upon the formation of the film. However, the Raman spectrum of aqueous metMb was restored once the Mb film was dissolved in a buffer solution. The NMR spectrum of the Mb solution prepared from the Mb film was also identical to that prepared from commercial Mb. We also recorded the Raman spectrum of as-received Mb dry powder using a 406.7 nm excitation (see Figure 2B). Even though the quality of the spectrum is not as good as that of Mb solution (or Mb film) due to a high background signal and use of a low excitation power, a higher intensity of band C (342 cm⁻¹) compared with band D and the presence of the spin marker band at 1587 cm⁻¹ indicate that the Fe in the dry powder is also in its low-spin state. This observation is further supported by the UV–visible absorption spectrum of the dry powder (see Figure 7B) which

(29) Ong, C. W.; Shen, Z. X.; Ang, K. K. H.; Kara, U. A. K.; Tang, S. H. *Appl. Spectrosc.* **1999**, *53*, 1097–1101.

(30) Ogoshi, H.; Saito, Y.; Nakamoto, K. *J. Chem. Phys.* **1972**, *57*, 4194–4202.

(31) Yamamoto, T.; Palmer, G.; Gill, D.; Salmeen, I. T.; Rimai, L. J. *Biol. Chem.* **1973**, *248*, 5211–5213.

(32) Tu, A. T. In *Raman Spectroscopy in Biology: Principles and Applications*; John Wiley & Sons Inc.: New York, 1982; pp 331–337.

(33) Kitagawa, T.; Kyogoku, Y.; Iizuka, T.; Saito, M. I. *J. Am. Chem. Soc.* **1976**, *98*, 5169–5173.

(34) Brunner, H.; Mayer, A.; Sussner, H. *J. Mol. Biol.* **1972**, *70*, 153–156.

(35) Desbois, A.; Lutz, M.; Banerjee, R. *Biochemistry* **1979**, *18*, 1510–1518.

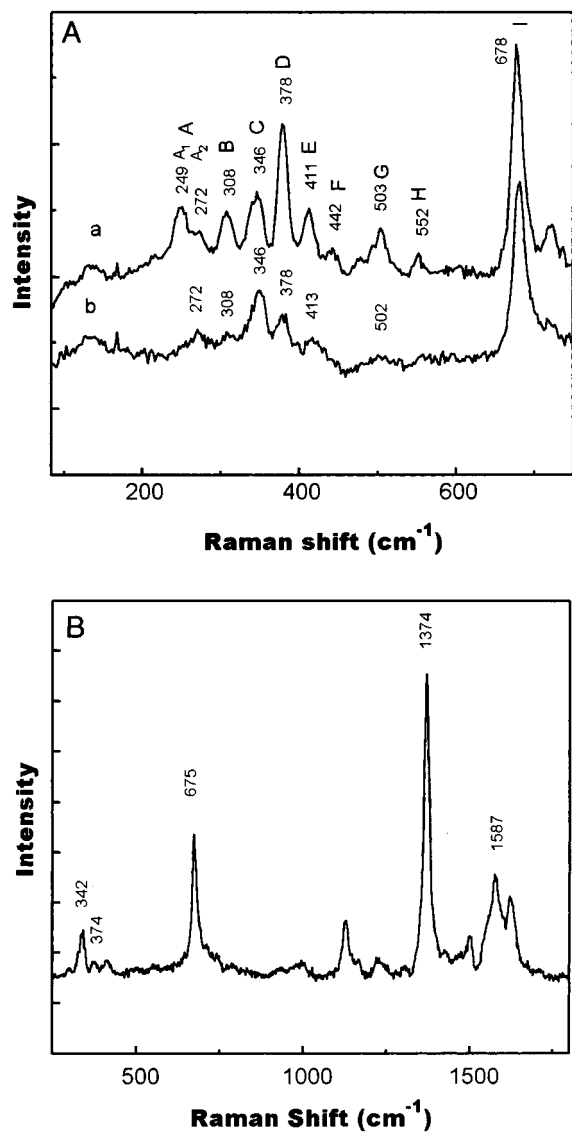


Figure 2. Resonance Raman spectra of (A) aqueous metMb (a) and Mb film (b) and (B) commercial Mb powder. $\lambda_{\text{ex}} = 406.7$ nm.

is characterized by the Soret band at 412 nm and α - β band at ~ 535 nm.

Origin of Spin State Change. When a strong field ligand (e.g. CN^- , CO, NO, etc.) coordinates with ferric Mb, the heme iron is in a low-spin state. So, the sixth position of the heme iron in the Mb film is most probably occupied by a strong ligand instead of water as in aqueous metMb. However, since no strong ligands exist in the buffer solution, the sixth position could only be occupied by an amino acid residue in the heme distal pocket. Figure 3a shows the structure of heme in the aqueous met Mb. The heme is coupled to peptide through the bond between the central iron and N on the imidazole ring of the histidine 93 residue (His93). On the distal side of the heme pocket, there is another histidine residue, histidine 64. Normally, this residue influences the binding properties of ligands to Mb both by sterically controlling access to the iron atom and by stabilizing the bound ligand through hydrogen bonding.^{25–27,36,37} X-ray diffraction shows that liganded and unliganded heme proteins possess different structures.^{38,39} The distal residue is forced to

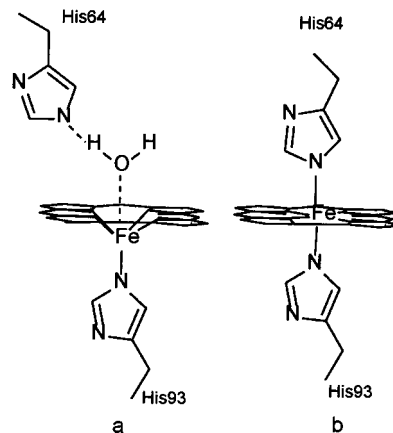


Figure 3. Structural diagrams of the heme of Mb: (a) aqueous metMb and (b) Mb film.

move into the solvent upon ligand (NO, imidazole) binding.^{40,41} Nienhaus and co-workers, using X-ray crystallography and time-resolved infrared spectroscopy, studied the conformational motions in Mb-carbon monoxide (MbCO mutant L29W) crystals induced by ligand dissociation.⁴² The authors claimed that the proteins fluctuated and transiently opened exit channels for ligands to escape from the distal pocket upon photodissociation above 180 K. The photoillumination above 180 K also caused rearrangements of the backbone in the vicinity of W29 and moved the H64 imidazole side chain deeper into the heme.

Water, a very weak ligand, binds to heme with the help of distal histidine in aqueous metMb, as shown in Figure 3a. As water evaporates from the system upon the formation of the Mb film, it may escape from the distal pocket owing to its weak coordination properties. The dissociation of water may result in the change of the heme distal pocket structure (see Figure 3b), as it does in MbCO upon photodissociation.⁴² Consequently, the N on the imidazole ring of H64 moves closer to the central iron and changes its spin state to low spin. However, when the Mb film is redissolved in buffer solution, water again competes with the imidazole group of H64 at the sixth position and forces the residue to move away from the heme iron. Therefore, the original distal pocket conformation for aqueous metMb is restored, thus the spin state of iron changes to high spin.

Raman Spectra of Mb-Imidazole Complex. To confirm the above conclusion, ferric Mb-imidazole complex solution was prepared in a phosphate buffer, and the Raman spectra of the complex were obtained by using 514.5 and 406.7 nm lines as the excitation source. The Raman spectrum of the complex with 514.5 nm excitation (Figure 4) was very similar to that of the Mb film with the same excitation. The bands, which appeared at 1210, 1565, and 1623 cm^{-1} in the spectrum of aqueous metMb, shifted to higher frequencies as they did for the Mb film. The Raman spectrum of the Mb-imidazole complex with a 406.7 nm excitation was also similar to that of the Mb film (see Figure 5i).

Effects of pH and Isotopic Substitution on Raman Spectra. Although it is most likely that the coordination of the N of H64 is responsible for the spin state change in the Mb film, there still exists the possibility that the spin state change arises from

(39) Phillips, S. E. V. *J. Mol. Biol.* **1980**, *142*, 531–554.

(40) Conti, E.; Moser, C.; Rizzi, M.; Mattevi, A.; Lionetti, C.; Coda, A.; Ascenzi, P.; Brunori, M.; Bolognesi, M. *J. Mol. Biol.* **1993**, *233*, 498–508.

(41) Lionetti, C.; Guanziroli, M. G.; Frigerio, F.; Ascenzi, P.; Bolognesi, M. *J. Mol. Biol.* **1991**, *217*, 409–412.

(42) Ostermann, A.; Waschipky, R.; Parak, F. G.; Nienhaus, G. U. *Nature* **2000**, *404*, 205–208.

(36) Mansy, S. S.; Olson, J. S.; Gonzalez, G.; Gilles-Gonzalez, M. A. *Biochemistry* **1998**, *37*, 12452–12457.

(37) Phillips, S. E. V.; Schoenborn, B. P. *Nature* **1981**, *292*, 81–82.

(38) Phillips, S. E. V. *Nature* **1978**, *273*, 247–248.

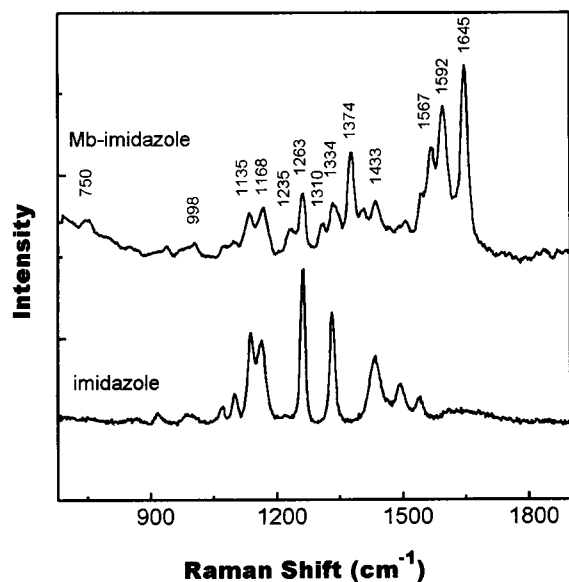


Figure 4. Resonance Raman spectra of Mb-imidazole complex. $\lambda_{\text{ex}} = 514.5$ nm.

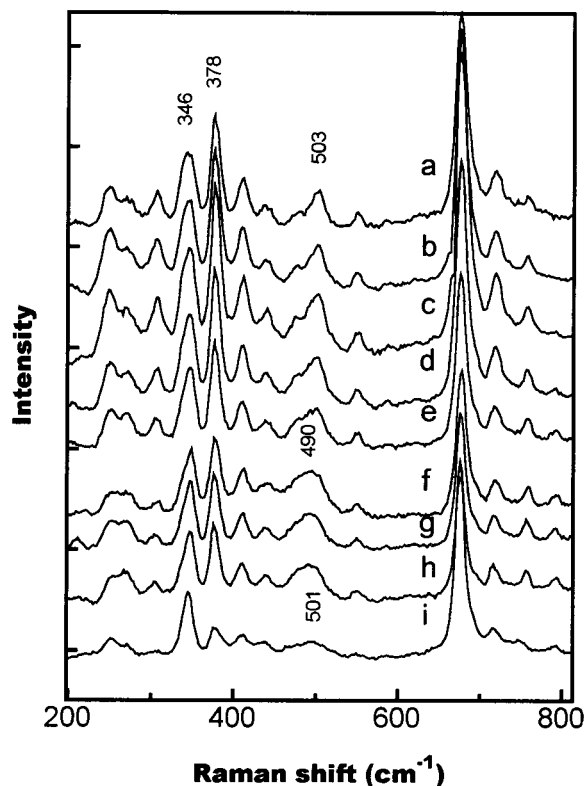


Figure 5. Resonance Raman spectra of aqueous Mb at pH values of (a) 7.5, (b) 8.1, (c) 8.6, (d) 9.1, (e) 9.6, (f) 10.3, (g) 10.6, and (h) 10.9 and (i) Mb-imidazole. $\lambda_{\text{ex}} = 406.7$ nm.

the coordination of OH^- ligand at the sixth position during the formation of Mb film. It is known that metMb, with a $\text{p}K_{\text{a}}$ of 8.6, is converted to a low-spin hydroxy derivative at a higher pH.⁴³ Even though the Mb film was formed from the Mb dissolved in pH 7.4 PB solution, stress during drying and (or) the microenvironment of the thin film might induce the formation of the hydroxy derivative. Figure 5 shows Raman spectra of Mb at various pH values in the range 7.4–10.9. As

(43) Antonini, E.; Brunori, M. In *Hemoglobin and Myoglobin in Their Reactions with Ligands*; North-Holland Publishing Company: London, 1971; Chapter 3, pp 50–54.

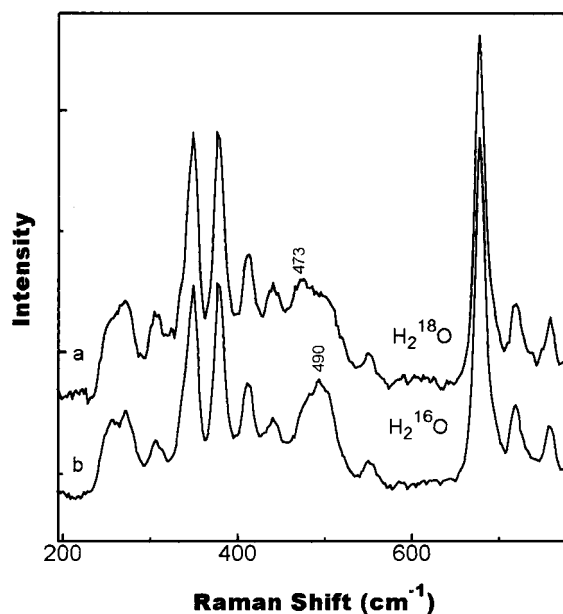


Figure 6. Resonance Raman spectra of Mb solutions (pH 10.5) prepared with H_2^{18}O (a) and H_2^{16}O (b). $\lambda_{\text{ex}} = 406.7$ nm.

described earlier, the intensity of band D (378 cm^{-1}) was higher than that of band C (346 cm^{-1}) in the neutral solution (pH 7.4). On the other hand, the ratio of the intensity of band C to D increased and a new band emerged at $\sim 490\text{ cm}^{-1}$ in solutions at higher pH values. This new band was reported to be “specific” for the hydroxy derivative.³⁵ Our isotopic substitution experiments also confirmed that this band is related to the coordination of OH^- . Figure 6 shows Raman spectra of Mb in H_2^{16}O and H_2^{18}O at pH 10.50. The substitution of ^{16}O by ^{18}O produced a $\sim 20\text{ cm}^{-1}$ shift in the OH^- specific band. This shift is basically the same as both experimental and theoretical shifts reported in the literature for this isotopic substitution.³⁵ We also recorded the Raman spectrum of the Mb film formed from Mb solution with H_2^{18}O and found that the spectrum was identical with that of the Mb film formed from H_2^{16}O ; neither the 490 cm^{-1} band nor the isotopic effect was observed. Therefore, it is unlikely that OH^- is the distal ligand in the film. Further experimental evidence to support this conclusion is the relative intensity of band C to D, which is reversely correlated with the molar susceptibility of Mb derivatives.³⁵ Since molar susceptibility of the hydroxy derivative is higher than that of the imidazole derivative, it is expected to have a lower intensity ratio of band C/D than that of the Mb-imidazole derivative. Since the Raman spectrum of the Mb film shows a high intensity ratio of band C/D which is similar to that in the Mb-imidazole spectrum (see Figure 5 spectrum i), H64 is a more likely distal ligand than OH^- .

UV-Vis Absorption Spectroscopy. UV-vis absorption spectroscopy was also used to correlate the spin-state change with the water evaporation and the imidazole coordination. Figure 7A shows a UV-vis absorption spectrum of the Mb-imidazole complex in the phosphate buffer, and Figure 7B shows spectra of the Mb film and Mb powder. Each figure also shows a spectrum of aqueous metMb for comparison. The intense absorption peak at 409 nm (Soret band) is a characteristic of high-spin metMb with water at the sixth position. Soret bands of the Mb film, Mb powder, and the Mb-imidazole complex were red shifted and appeared at 412–413 nm suggesting that E7 histidine is coordinated to the sixth position of the heme iron in the Mb film. The α - β bands were also red shifted upon

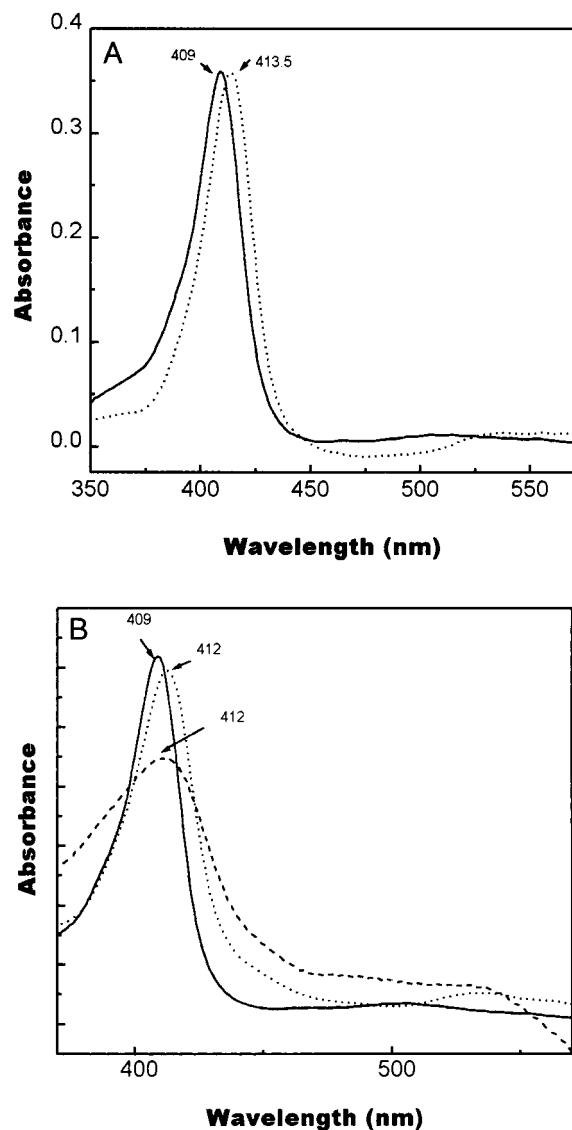


Figure 7. UV-vis absorption spectra of (A) metMb (solid line) and Mb-imidazole complex (dotted line) in a pH 7.4 phosphate buffer and (B) metMb (solid line) in a pH 7.4 phosphate buffer, Mb film on quartz plate (dotted line), and as-received Mb powder (dash line).

formation of the Mb film or the low-spin Mb-imidazole complex.

Cyclic Voltammetry. It is suggested that electron transfer between the heme iron and electrode or chemical reductant is through the sixth ligand or through the porphyrin ring;^{44,45} ligands which possess a $p\pi$ orbital normally provide an effective pathway for the electron transfer due to the overlaps of the $p\pi$ orbital with the d orbital of iron. The rate of direct reduction of ferric Mb coordinating with different ligands⁴⁴ by sodium dithionite differs by many orders of magnitude and follows the order of imidazole \gg $CN^- > SCN^- \gg N_3^- \gg F^-$. The high reduction rates of the Mb-imidazole and other low-spin complexes are due to their $p\pi$ orbitals which provide a route for the electron transfer. It was reported that the rate of heterogeneous electron transfer between the tin-doped indium oxide electrode and the proteins increased by 1 order of magnitude⁴⁵ when metMb (with water at the sixth position) was converted to cyanometmyoglobin. Since the water molecule also

possesses a $p\pi$ orbital, the rate of electron transfer between aqueous metMb and the electrode should be similar to that of cyanometmyoglobin. The difference in the observed electron-transfer rate was attributed to the different spin state involved in the two redox couples.⁴⁵ In high-spin metMb, the iron has a larger radius and lies 0.4 Å below the heme plane toward H93, and the porphyrin ring is domed (or described as puckered). On the other hand, in the low-spin state the radius of iron is smaller and can fit into the porphyrin ring. For a redox couple involving two different spin states, the length of the Fe-N bond and the conformation of heme group may change when the oxidation state is changed. The reorganization energy change involved in the electron-transfer reaction between these states will exceed that for the analogous electron-transfer reaction which involves the same spin state.^{46,47} As a result the heterogeneous electron-transfer rate of heme protein redox couples involving various combinations of spin states follows the order of low-spin/low-spin $>$ high-spin/high-spin \gg high-spin/low-spin or low-spin/high-spin.⁴⁵

Another factor that may contribute to the rate of heterogeneous electron transfer of Mb is the distal-pocket H-bonding network. Armstrong and co-workers⁴⁸ reported a significant improvement in electron-transfer kinetics when the H64 of sperm-whale myoglobin was replaced by such residues as valine, leucine, methionine, glycine, or phenylalanine. They showed well-behaved voltammograms of H64 mutants contrary to that of wild-type Mb which was characterized by having poorly defined waves with a large potential separation. The difference in electrochemical behavior between WT-Mb and the mutants was attributed to the alteration of the distal pocket H-bonding network, which extends from the interior of the distal heme pocket in the WT-Mb to the heme periphery and the bulk solution.⁴⁹ This H-bonding network was considered to increase the electron-transfer activation energy by coupling the displacement of Fe(III)-coordinated H_2O to the more demanding reorganization of bulk H_2O . Since the H-bonding network no longer exists in H64 mutants, these proteins showed a well-behaved voltammogram due to the increase of the rate of heterogeneous electron transfer.

In the proposed conformation of the Mb film, the position for an exogenous ligand at the distal side of the heme iron is now occupied by the imidazole side chain, and the iron atom is pulled into the heme plane which makes the porphyrin ring flat and the iron in a low-spin state. Since the reduced form of Mb with imidazole at the sixth position is still low spin, the reduction of the Mb film should result in a slight change of the iron radius and heme conformation that should provide a higher heterogeneous electron-transfer rate. Furthermore, since the distal water no longer coordinates to the heme iron and the H-bonding network does not exist, one expects an increase of corresponding electron-transfer rate as is the case for the H64 mutants. This assumption was supported by electrochemical experiments. To prevent the film from dissolving and converting the protein to high-spin metMb, the film was covered with a thin layer of Nafion. Raman and reflectance absorbance IR spectra of the Mb film (amide I,II bands) recorded before and after covering with Nafion showed no difference. The results indicate that the helical structure of the polypeptide and the environment surrounding the heme group remained the same as those of the

(46) Tsukahara, K.; Okazawa, T.; Takahashi, H.; Yamamoto, Y. *Inorg. Chem.* **1986**, *25*, 4756-4760.

(47) Kadish, K. M.; Su, C. H. *J. Am. Chem. Soc.* **1983**, *105*, 177-180.

(48) Van Dyke, B. R.; Saltman, P.; Armstrong, F. A. *J. Am. Chem. Soc.* **1996**, *118*, 3490-3492.

(49) Quillin, M. L.; Arduini, R. M.; Olson, J. S.; Phillips, G. N., Jr. *J. Mol. Biol.* **1993**, *234*, 140-155.

(44) Cox, R. P.; Hollaway, M. R. *Eur. J. Biochem.* **1977**, *74*, 575-587.
(45) King, B. C.; Hawkrige, F. M.; Hoffman, B. M. *J. Am. Chem. Soc.* **1992**, *114*, 10603-10608.

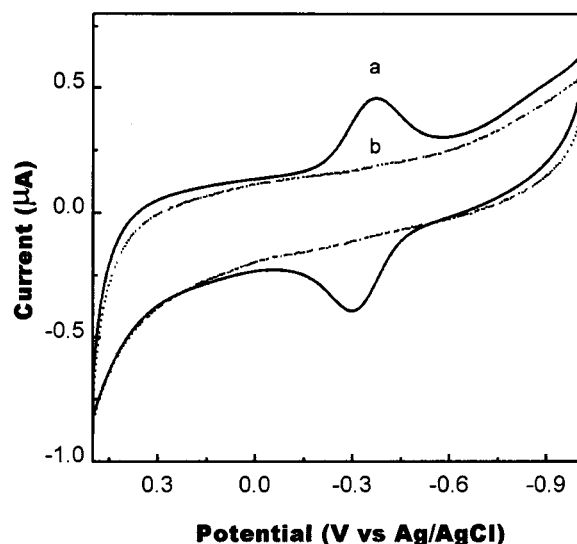


Figure 8. Cyclic voltammograms of (a) the Mb film electrode in a pH 7.4 phosphate buffer and (b) a bare glassy carbon electrode in a buffer solution containing 5×10^{-4} M metMb. Scan rate = 0.1 V/s.

Mb film without Nafion. Raman spectroscopy also showed that the heme iron in the Mb film covered with Nafion remained low spin, even when the Mb film was wet in the buffer solution. The results may be explained by noting that the relatively “rigid” Nafion matrix restricted the restoration of Mb in the film and (or) the concentration of water in the film was much lower and could not compete with the H64 side chain for the sixth coordination position of the heme iron.

The heterogeneous electron transfer between the aqueous metMb and a bare electrode such as Au, Pt, and carbon electrodes is known to be very slow.¹⁰ As expected, the anodic and the cathodic peak were hardly observed in the CV of the metMb solution at the GC electrode in the present study. However, when the electrode was covered with an Mb–Nafion film or metMb was converted to the Mb–imidazole complex, the electron-transfer rate was significantly increased. Figure 8a shows a CV of the Mb film on a GC electrode in a pH 7.4 phosphate buffer (0.1 M) containing 0.1 M NaCl at a scan rate of 0.1 V/s. A well-behaved voltammogram was observed with a midpoint potential ($E_{1/2}$) at -0.34 V which was ~ 160 mV more negative than the reported formal potential of Mb in a buffer solution.⁵⁰ Cyclic voltammetry also showed that the anodic peak current was lower than that of the cathodic peak current at slow scan rates,⁵¹ but the ratio of the anodic peak current to the cathodic peak current increased by increasing the scan rate. The results may suggest the involvement of an EC mechanism due to the dissociation of imidazoles from the sixth position after the reduction of an heme iron.

Figure 9 shows a CV of an aqueous Mb–imidazole complex at a bare GC electrode. The midpoint potential for the redox reaction of heme iron was -0.38 V, and the ratio of the anodic to the cathodic peak current again increased with increasing scan rate. However, the ratio of the anodic to the cathodic peak for an aqueous Mb–imidazole complex was much lower than that for the Mb film when recorded at a scan rate of 0.1 V/s. This implies that the dissociation of free imidazole from ferrous Mb is faster than that of the H64 imidazole group that bonded to the apomyoglobin backbone. A likely reason for the difference in dissociation is that the variation in position of H64 imidazole

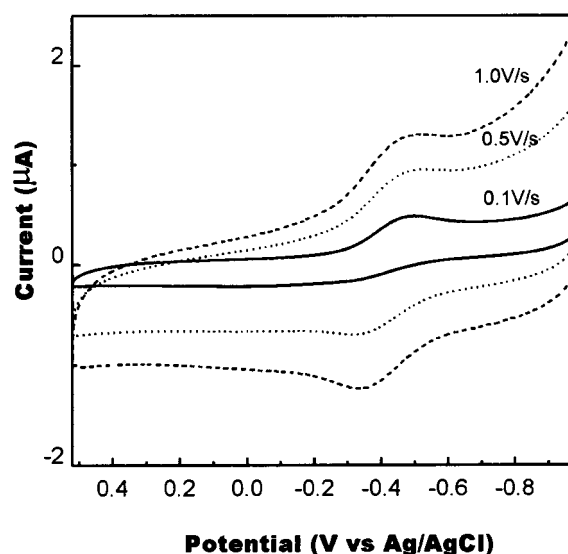


Figure 9. Cyclic voltammograms of the Mb–imidazole complex in a pH 7.4 phosphate buffer at different scan rates.

is restricted by the polypeptide backbone. Since the escape of the imidazole group from the distal site of ferrous iron may be slowed by the polypeptide backbone in the Mb film, the equilibrium cannot be reached and most of the H64 side chain is still coordinated to Fe(II) during the fast potential scan. The negatively shifted midpoint potentials of both the Mb film and Mb–imidazole complex indicate that similarly coordinated heme irons are involved in these two redox couples in which the ferric Mb has the greater affinity for the H64 side chain (or imidazole) than the ferrous Mb.^{44,45} The less negatively shifted midpoint potential of the Mb film indicates that interaction between the iron atom and the distal ligand in the Mb film is weaker than that of imidazole and Mb in the derivative.

Reflectance Absorbance Infrared Spectroscopy. Raman and UV–vis spectra are mainly used for providing information on ligand coordination features and the heme pocket structure. The displacement of H64 imidazole in the film may result from either a slight conformational change in the heme distal pocket or complete helical conformation changes of the polypeptide chain. IR spectra of Mb mainly arise from vibrational modes of the polypeptide amide bond and, thus, can be related to the helical structure of the protein. Reflectance absorbance infrared spectra of both as-received Mb and the Mb film on a gold surface are shown in Figure 10. The amide I and II bands are basically identical in the two spectra, indicating little change in the protein helical structure during the formation of the Mb film.⁹ The only notable difference in these spectra is that the relative intensity of the band at 1102 cm^{-1} from the Mb film is slightly higher than that from the as-received Mb sample. This might suggest some form of conformational change involving the polypeptide upon the formation of the Mb film which requires further investigation.

Conclusions

Raman spectra recorded with a 514.5 nm excitation show that the spin marker bands in the 1550 – 1630 cm^{-1} region were shifted ~ 20 cm^{-1} to higher frequencies upon the formation of the Mb film. This indicates that the spin state of Mb was changed from high to low when the Mb film was formed from an aqueous metMb solution. The Raman spectroscopy also indicates that the iron atom in the Mb film lies in the heme plane rather than being displaced by ~ 0.4 Å out of the heme

(50) (a) Faulkner, K. M.; Bonaventura, C.; Crumbliss, A. L. *J. Biol. Chem.* **1995**, *270*, 13604. (b) Taylor, J. F. *J. Biol. Chem.* **1944**, *144*, 7.

(51) Chou, J.; Tachikawa, H. Unpublished results.

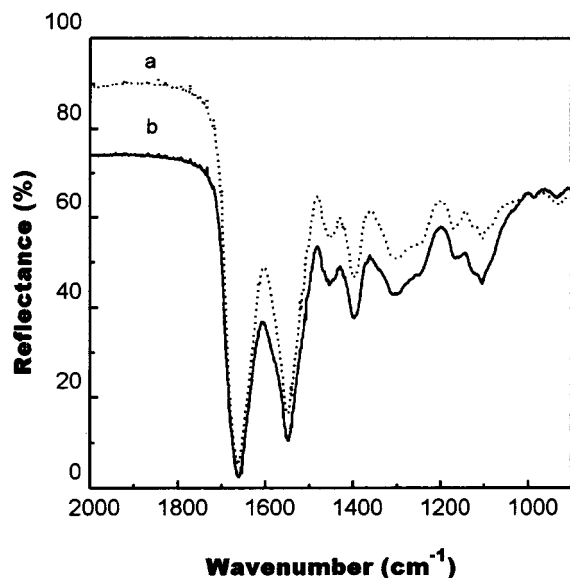


Figure 10. Reflectance absorbance IR spectra of Mb: (a) as-received Mb and (b) Mb film.

plane which is the case for aqueous metMb. A low-frequency region of the Raman spectra recorded with a 406.7 nm excitation also shows a spectral feature that supports the above conclusion. The results obtained by the UV-vis absorption spectroscopy

are also consistent with the Raman data indicating that the iron in the Mb film is low spin. Both the pH and isotopic substitution studies on Raman spectra showed that the low-spin hydroxyl derivative was not formed in the Mb film. A comparison of the Raman spectra of the Mb film with those of the Mb-imidazole complex indicates that the features of these two Raman spectra are very similar, and the coordination of H64 to the sixth position of iron is very likely in the Mb film. This conformation should reduce the electron-transfer activation energy due to the absence of the distal pocket H-bonding network and favor a fast electron transfer. Another factor contributing to the fast electron transfer is that both ferric and ferrous iron in the Mb film are low spin which should involve a smaller reorganizational energy change during the redox reaction. This structural feature of the heme in the Mb film, having a low-spin state and the iron atom being in the heme plane, favors fast heterogeneous electron transfer between the protein and the electrode. The reflectance absorbance FT-IR spectroscopy shows that the essential features of the native structure of Mb were maintained upon the formation of the Mb film.

Acknowledgment. This work was supported in part by the National Institutes of Health (Grant SO6GMO8047). The authors thank Professor Xiaotang Wang of Jackson State University for valuable discussions.

JA003088P